*Publ. Astron. Soc. Japan* (2018) 70 (5), L7 (1–5)
doi: 10.1093/pasj/psy102
Advance Access Publication Date: 2018 September 18

# A search for optical transients associated with fast radio burst 150418†‡

**Yuu NIINO,[1,*] Nozomu TOMINAGA,[2,3] Tomonori TOTANI,[4,5] Tomoki MOROKUMA,[6] Evan KEANE,[7] Andrea POSSENTI,[8] Hajime SUGAI,[3] and Shotaro YAMASAKI[4]**

[1]National Astronomical Observatory of Japan, 2-21-1 Osawa, Mitaka, Tokyo 181-8588, Japan
[2]Department of Physics, Faculty of Science and Engineering, Konan University, 8-9-1 Okamoto, Kobe, Hyogo 658-8501, Japan
[3]Kavli Institute for the Physics and Mathematics of the Universe (WPI), The University of Tokyo Institutes for Advanced Study, 5-1-5 Kashiwa-no-Ha, Kashiwa, Chiba 277-8583, Japan
[4]Department of Astronomy, School of Science, The University of Tokyo, 7-3-1 Hongo, Bunkyo-ku, Tokyo 113-0033, Japan
[5]Research Center for the Early Universe, School of Science, The University of Tokyo, 7-3-1 Hongo, Bunkyo-ku, Tokyo 113-0033, Japan
[6]Institute of Astronomy, Graduate School of Science, The University of Tokyo, 2-21-1 Osawa, Mitaka, Tokyo 181-0015, Japan
[7]SKA Organisation, Jodrell Bank Observatory, Cheshire SK11 9DL, UK
[8]INAF-Osservatorio Astronomico di Cagliari, Via della Scienza 5, I-09047 Selargius (CA), Italy

*E-mail: yuu.niino@nao.ac.jp

†Based on data collected at Subaru Telescope, which is operated by the National Astronomical Observatory of Japan.
‡Based on observations obtained at the Gemini Observatory acquired through the Gemini Observatory Archive, which is operated by the Association of Universities for Research in Astronomy, Inc., under a cooperative agreement with the NSF on behalf of the Gemini partnership: the National Science Foundation (United States), the National Research Council (Canada), CONICYT (Chile), Ministerio de Ciencia, Tecnología e Innovación Productiva (Argentina), and Ministério da Ciência, Tecnologia e Inovação (Brazil).

Received 2018 June 2; Accepted 2018 August 9

## Abstract

We have searched for optical variability in the host galaxy of the radio variable source possibly associated with fast radio burst (FRB) 150418. We compare images of the galaxy taken 1 day after the burst using Subaru/Suprime-Cam with images taken $\sim$1 yr after the burst using Gemini-South/GMOS. No optical variability is found between the two epochs with a limiting absolute magnitude $\gtrsim -19$ (AB). This limit applies to the optical variability of the putative active galactic nucleus in the galaxy on a timescale of $\sim$1 yr, and also to the luminosity of an optical counterpart of FRB 150418 one day after the burst should it have occurred in this galaxy.

**Key words:** galaxies: active — radio continuum: general — supernovae: general

## 1 Introduction

Fast radio burst (FRB) 150418 was detected by the Parkes radio telescope at 04:29:07 on 2015 April 18 (UTC; Keane et al. 2016). A multiwavelength follow-up campaign was conducted with various telescopes including the Australia Telescope Compact Array (ATCA; 5.5 GHz and 7.5 GHz) and Subaru (optical, *r* and *i* bands). A fading radio object with a negative spectral index ($f_\nu \propto \nu^{-1.37}$) was detected by ATCA within the error circle of FRB 150418 in the first 6 d after the burst. This led to a claimed association between the source and FRB 150418; however, it is possible that the fading source is scintillation of radio emission from an active galactic nucleus (AGN) and unrelated to FRB 150418 (Williams & Berger 2016; Akiyama & Johnson 2016; Johnston et al. 2017).

Optical imaging observations of the error circle of FRB 150418 using Suprime-Cam (Miyazaki et al. 2002) on the Subaru telescope were conducted 1 to 2 d after the burst. Although no peculiar variable object was found within the error circle, an early-type galaxy was clearly detected at the position of the fading object observed by ATCA. The galaxy has also been detected by the WISE satellite (Wright et al. 2010) and catalogued as WISE J071634.59−190039.2 (hereafter WISE J0716−19). Subsequent spectroscopy of WISE J0716−19 using Subaru/FOCAS (Kashikawa et al. 2002) revealed that its redshift is $z = 0.492 \pm 0.008$ (Keane et al. 2016).

No variable object was found in WISE J0716−19 in the optical images taken with Suprime-Cam 1 to 2 d after the burst. However, an optical counterpart of FRB 150418 might be missed by those observations even if it existed at the time of observation, if the variability timescale of the optical counterpart is longer than the observation period. In this study we compare the images taken 1 to 2 d after the burst with images of the same field taken ~1 yr after the burst using GMOS on Gemini-South (Hook et al. 2004), to search for any optical transient event that may have occurred in WISE J0716−19 during the period between the two observations. Throughout the paper we assume the fiducial cosmology with $\Omega_\Lambda = 0.7$, $\Omega_m = 0.3$, and $H_0 = 70\,\mathrm{km\,s^{-1}\,Mpc^{-1}}$. Magnitudes are given in the AB system.

## 2 Data

Our optical follow-up observations of FRB 150418 using Subaru/Suprime-Cam were performed on 2015 April 19 and 20 UTC (Keane et al. 2016; hereafter "the event images"). To detect any optical variability of WISE J0716−19 with timescale longer than ~1 d we retrieved GMOS observations of WISE J0716−19 conducted ~1 yr after the burst from the Gemini observatory archive as reference images (Program ID: GS-2016A-Q-104). The reference images were taken under lightly cloudy conditions (CC = 70%-tile).[1]

The event images were reduced using the Hyper-Suprime-Cam pipeline version 3.8.5 (Bosch et al. 2018), which is based on the LSST pipeline (Ivezic et al. 2008; Axelrod et al. 2010), and the reference images were reduced using PyRAF/IRAF,[2] together with the Gemini IRAF package.

We summarize information about the observations in table 1. In the following discussions we use the event images obtained on 2015 April 19 and the reference images obtained on 2016 March 15, due to the poor seeing conditions on 2015 April 20 and 2016 April 11. The 80 × 80 arcsec$^2$ field centered on WISE J0716−19 in the *i* band is shown in figure 1. We calibrated the flux scale of the event images using unsaturated objects in the same field that are catalogued in the Pan-STARRS1 database (Chambers et al. 2016) as photometric standards.

## 3 Search for a variable object

### 3.1 Relative photometry between the two epochs

To achieve accurate relative photometry between the two epochs we compared photon counts of unsaturated objects in the field, and calibrated the flux scale of the reference images so that the fluxes of the unsaturated objects are the same as those in the event images. We performed photometry of objects in the images using the SExtractor software (Bertin & Arnouts 1996).

In figure 2 we show the flux ratios of the unsaturated objects between the event and reference images as a function of their flux densities in the event image. As expected, the flux ratios of fainter objects are more scattered. Furthermore, there is a systematic error where faint objects appear systematically brighter in the reference image in the *i* band. To avoid any unwanted impact of faint objects on the photometry, we used objects at least 50% as bright as WISE J0716−19 for the photometric calibration.

WISE J0716−19 is shown with a star symbol in figure 2. Although significant change in the flux density of WISE J0716−19 is not found in the *i* band, the flux density has decreased in the *r* band by 20% between the two epochs. The measured flux densities of WISE J0716−19 in the event

[1] ⟨http://www.gemini.edu/sciops/telescopes-and-sites/observing-condition-constraints⟩.

[2] PyRAF is a product of the Space Telescope Science Institute, which is operated by AURA for NASA. IRAF is distributed by the National Optical Astronomy Observatories, which are operated by the Association of Universities for Research in Astronomy, Inc., under cooperative agreement with the National Science Foundation.

**Table 1.** Observations of WISE J0716−19.

| Start time (UTC) | Telescope/instrument | Filter | Exposures | Seeing |
|---|---|---|---|---|
| 2015 April 19 05:58:27 | Subaru/Suprime-Cam | *i*-band | 60 s × 10 | 0.″7 |
| 2015 April 19 06:25:07 | Subaru/Suprime-Cam | *r*-band | 60 s × 15 | 0.″7 |
| 2015 April 20 05:35:39 | Subaru/Suprime-Cam | *i*-band | 60 s × 20 | 0.″9 |
| 2015 April 20 06:15:46 | Subaru/Suprime-Cam | *r*-band | 60 s × 20 | 1.″2 |
| 2016 March 15 02:13:08 | Gemini-South/GMOS | *r*-band | 150 s × 7 | 0.″7 |
| 2016 March 15 02:35:14 | Gemini-South/GMOS | *i*-band | 150 s × 7 | 0.″6 |
| 2016 April 11 00:08:20 | Gemini-South/GMOS | *z*-band | 150 s × 7 | 0.″9 |
| 2016 April 11 00:30:34 | Gemini-South/GMOS | *i*-band | 150 s × 7 | 0.″9 |

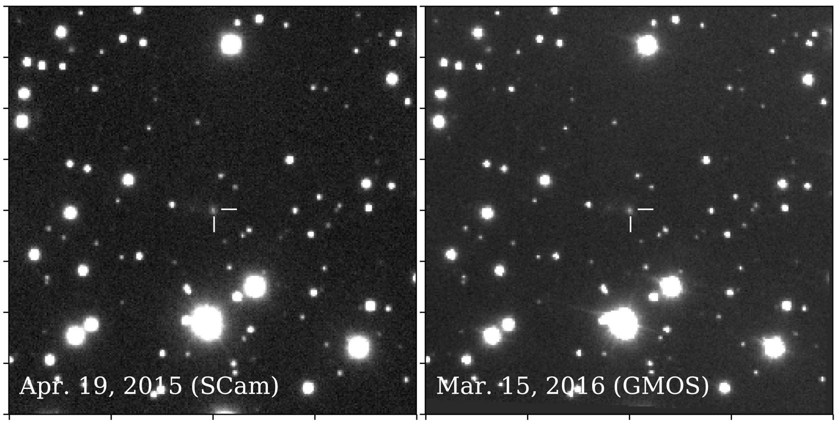


**Fig. 1.** Left panel: 80″ × 80″ field image in the *i* band centered on WISE J0716−19, which is highlighted with cross hairs. North is up, east to the left. The image was taken on 2015 April 19 using Subaru/Suprime-Cam (the event image). Right panel: Same as the left panel but taken on 2016 March 15 using Gemini-South/GMOS (the reference image). The pixels were aligned with those of the event image using the `remap` program in WCSTools.

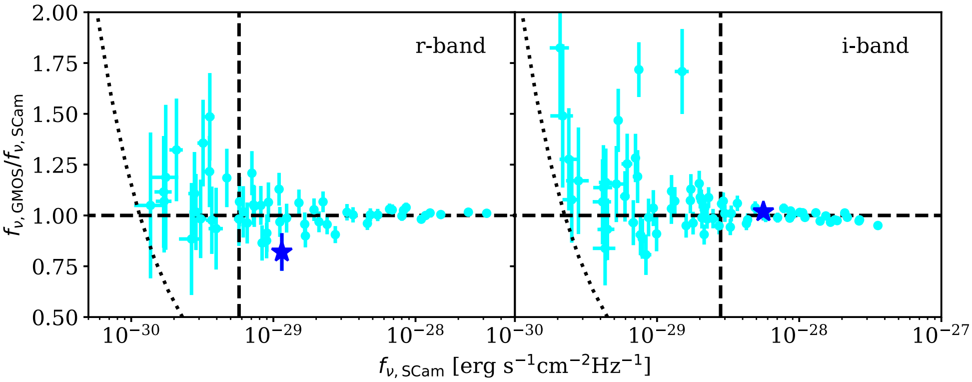


**Fig. 2.** Flux ratios of objects in the vicinity of WISE J0716−19 between the event and reference images in the *r* and *i* bands (the left and right panels, respectively). The error bars are 1 $\sigma$ significance. WISE J0716−19 is shown with a star symbol. The vertical dashed line indicates the lower flux limit above which objects are used for the calibration of relative photometry, and the horizontal dashed line indicates $f_{\nu,\,\mathrm{GMOS}}/f_{\nu,\,\mathrm{SCam}} = 1.0$. The dotted curve represents a constant $f_{\nu,\,\mathrm{GMOS}}$. One of the two outliers with $f_{\nu,\,\mathrm{GMOS}}/f_{\nu,\,\mathrm{SCam}} > 1.5$ at $f_{\nu,\,\mathrm{SCam}} \sim 10^{-29}$ erg s$^{-1}$ cm$^{-2}$ Hz$^{-1}$ in the right panel is a diffuse object which may suffer from uncertainty in the aperture determination, and the other one is blended with a nearby bright object. (Color online)

and reference images by SExtractor are $(1.15 \pm 0.07) \times 10^{-29}$ and $(0.94 \pm 0.09) \times 10^{-29}$ erg s$^{-1}$ cm$^{-2}$ Hz$^{-1}$, respectively. However, this difference likely results from extra errors in the photometry that are not taken into account in the error estimation by SExtractor, such as uncertainty of aperture determination. We ran SExtractor independently on the event and reference images because the pixel alignments are different between the images, and the elliptical

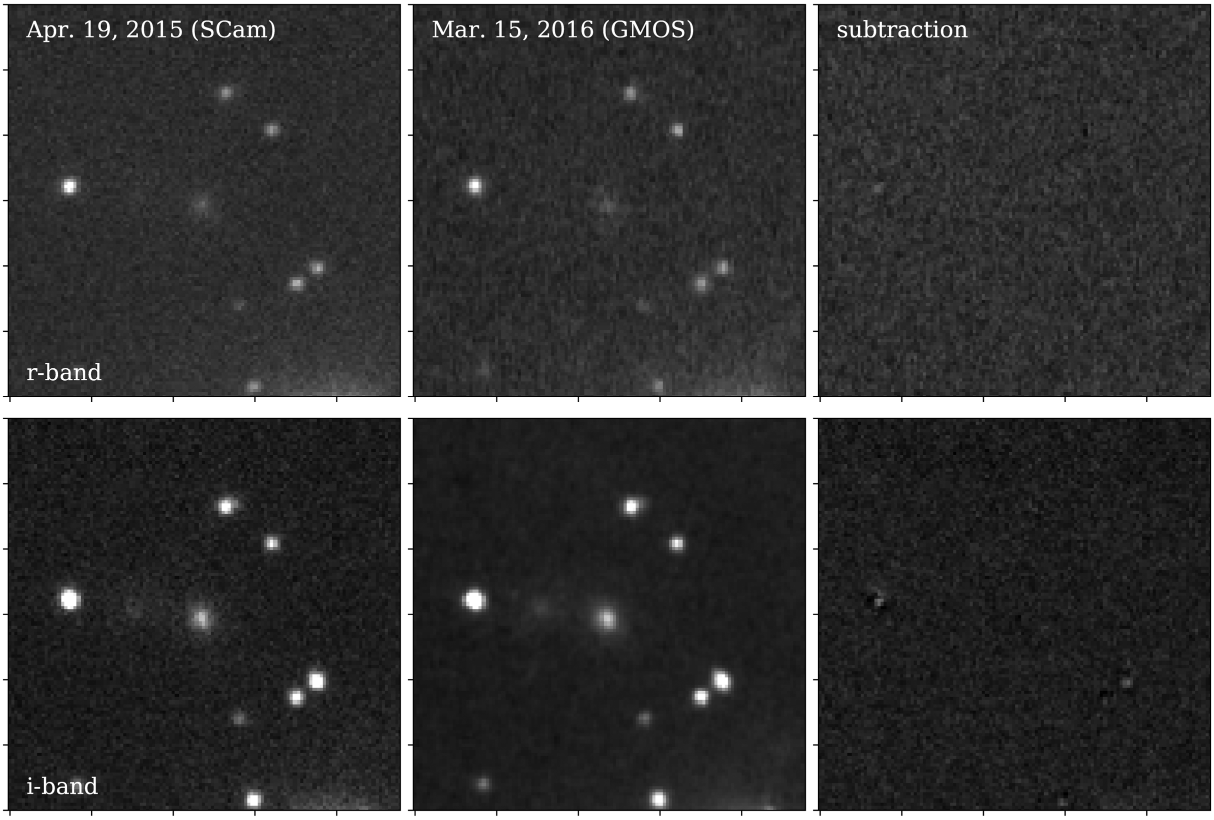


**Fig. 3.** Left and middle panels: As figure 1 but zoomed in to a 24″ × 24″ region centered on WISE J0716−19. The upper and lower panels are the images in the *r* and *i* bands, respectively. Right panels: Subtraction of the reference images (the middle panels) from the event images (the left panels).

aperture for WISE J0716−19 determined by SExtractor is different in each image. To examine the dependence of the flux density on the determination of the photometric aperture, we performed photometry of WISE J0716−19 in the *r* band with circular apertures of various diameters between 3″ and 7″ with a sampling rate of 0.″1, instead of the elliptical aperture determined by SExtractor.

The mean and the root-mean-square error of the flux densities obtained in this range of aperture diameters are $(1.13 \pm 0.13) \times 10^{-29}\,\mathrm{erg\,s^{-1}\,cm^{-2}\,Hz^{-1}}$ in both the event and reference images. Thus, we conclude that the decrease of the flux density in the *r* band seen in figure 2 is not real. We also note that WISE J0716−19 is an extended source while most of the other objects in the field are point sources, and hence it suffers more from the uncertainty in the aperture determination than other objects, and a faint object that resides ∼5″ east of WISE J0716−19 may also affect the photometry.

## 3.2 Image subtraction

To search for a transient object in WISE J0716−19, we subtracted the calibrated reference images from the event images. We used the `remap` program in WCSTools[3] to align the pixels of the reference images obtained using GMOS-S (0.″16 per pixel) with that of the event images obtained by Suprime-Cam (0.″20 per pixel). We also convolved the *i*-band reference image with a Gaussian kernel to make the point spread function (PSF) size consistent with that of the event image.

The images of WISE J0716−19 with the two filters at the two epochs and the subtracted images are shown in figure 3. No residual source is visible at the position of WISE J0716−19 in the subtracted images. To estimate the detection limits of the subtraction images we randomly distributed a thousand circular apertures 1.″4 in diameter (twice the full width at half maximum of the PSF) on blank fields in the subtracted images, and investigated the distributions of the flux densities in those apertures. The $3\,\sigma$ scatter of the obtained distributions is $1.51 \times 10^{-30}$ and $1.65 \times 10^{-30}\,\mathrm{erg\,s^{-1}\,cm^{-2}\,Hz^{-1}}$ in the *r* and *i* bands, respectively, which we consider as the upper limits on a transient object that was occurring in WISE J0716−19 at the time the event images were taken.

[3] ⟨http://tdc-www.cfa.harvard.edu/software/wcstools/⟩.

To confirm the nonexistence of a variable source in WISE J0716−19 quantitatively we performed aperture photometry with circular apertures of 1.″4 in diameter at the position of WISE J0716−19 on the subtracted images. The resulting flux densities are $2.64 \times 10^{-31}$ and $-1.06 \times 10^{-31}\,\mathrm{erg\,s^{-1}\,cm^{-2}\,Hz^{-1}}$ in the $r$ and $i$ bands, respectively, which is consistent with the limits derived above.

## 4 Discussion

Taking account of the redshift $z = 0.492$ of WISE J0716−19 and correcting for the large foreground extinction of $A_V = 3.7$ in the direction (Schlafly & Finkbeiner 2011), the upper limits derived in the previous section correspond to absolute magnitudes of $>-19.4$ and $>-18.7$ at rest-frame wavelengths of 4200 and 5100 Å, respectively. The absolute limiting magnitudes are fainter than peak magnitudes of type Ia supernovae (SNe) and broad-lined type Ic SNe, while they are brighter than most type II SNe even at the peak of their lightcurve (e.g., Barbary et al. 2012; Dahlen et al. 2012; Okumura et al. 2014; Whitesides et al. 2017). However, the peak time of a SN lightcurve is typically ∼10 d after the burst. Taking into account that the event images were taken 1 d after the occurrence of FRB 150418, association of a SN of any type with FRB 150418 is not ruled out even if FRB 150418 really occurred in WISE J0716−19.

Unlike a SN, an optical afterglow of a gamma-ray burst (GRB) usually reaches its peak luminosity within 1 d of the burst—for reviews of the observational properties of GRB optical afterglows, see Kann et al. (2011) and references therein. The absolute limiting magnitudes derived above are comparable to luminosities of the short GRB afterglows 1 d after the bursts (optical absolute magnitude ∼−21 to −18), and hence an afterglow could have been observed if a short GRB (or a long GRB, whose afterglow is typically brighter) occurred in WISE J0716−19 simultaneously with FRB 150418. It has also been pointed out that the energy of the outflowing material is comparable to that of a short GRB, if the ATCA object is a similar phenomenon to a GRB afterglow (Zhang 2016). However, an afterglow would not be visible when the GRB event is off-axis. We also note that optical afterglows are not detected for many short GRBs, and the sample of short GRB afterglows with known luminosity may represent the bright end of the overall population. Thus, the occurrence of a GRB in WISE J0716−19 is not ruled out.

The radio emission of WISE J0716−19 suggests that it hosts a radio-faint AGN (Williams & Berger 2016; Vedantham et al. 2016; Bassa et al. 2016; Giroletti et al. 2016; Johnston et al. 2017). However, the optical spectrum of WISE J0716−19 shows no AGN signature (Keane et al. 2016), suggesting that the disk luminosity of any putative AGN is low. Our non-detection of any optical variability also supports this interpretation.

The constraints on the optical variability of WISE J0716−19 are weak, largely due to the foreground extinction of $A_V = 3.7$. Optical follow-up observations of FRBs at higher Galactic latitudes where extinction in the Milky Way is small are desired to search for an optical counterpart of a FRB.

## Acknowledgments

We thank the anonymous referee for his/her helpful comments. This work was supported by JSPS KAKENHI Grant Number JP17K14255.

## References

Akiyama, K., & Johnson, M. D. 2016, ApJ, 824, L3
Axelrod, T., Kantor, J., Lupton, R. H., & Pierfederici, F. 2010, in Proc. SPIE, 7740, Software and Cyberinfrastructure for Astronomy, ed. N. M. Radziwill & A. Bridger (Bellingham, WA: SPIE), 774015
Barbary, K., et al. 2012, ApJ, 745, 31
Bassa, C. G., et al. 2016, MNRAS, 463, L36
Bertin, E., & Arnouts, S. 1996, A&AS, 117, 393
Bosch, J., et al. 2018, PASJ, 70, S5
Chambers, K. C., et al. 2016, arXiv:1612.05560
Dahlen, T., Strolger, L.-G., Riess, A. G., Mattila, S., Kankare, E., & Mobasher, B. 2012, ApJ, 757, 70
Giroletti, M., Marcote, B., Garrett, M. A., Paragi, Z., Yang, J., Hada, K., Muxlow, T. W. B., & Cheung, C. C. 2016, A&A, 593, L16
Hook, I. M., Jørgensen, I., Allington-Smith, J. R., Davies, R. L., Metcalfe, N., Murowinski, R. G., & Crampton, D. 2004, PASP, 116, 425
Ivezic, Z., et al. 2008, arXiv:0805.2366
Johnston, S., et al. 2017, MNRAS, 465, 2143
Kann, D. A., et al. 2011, ApJ, 734, 96
Kashikawa, N., et al. 2002, PASJ, 54, 819
Keane, E. F., et al. 2016, Nature, 530, 453
Miyazaki, S., et al. 2002, PASJ, 54, 833
Okumura, J. E., et al. 2014, arXiv:1401.7701
Schlafly, E. F., & Finkbeiner, D. P. 2011, ApJ, 737, 103
Vedantham, H. K., Ravi, V., Mooley, K., Frail, D., Hallinan, G., & Kulkarni, S. R. 2016, ApJ, 824, L9
Whitesides, L., et al. 2017, ApJ, 851, 107
Williams, P. K. G., & Berger, E. 2016, ApJ, 821, L22
Wright, E. L., et al. 2010, AJ, 140, 1868
Zhang, B. 2016, ApJ, 822, L14